Neural Computing and Applications (2018) 30:2017–2028
https://doi.org/10.1007/s00521-018-3489-y

S.I. : DEEP LEARNING FOR BIOMEDICAL AND HEALTHCARE APPLICATIONS

A lossless data hiding scheme for medical images using a hybrid solution based on IBRW error histogram computation and quartered interpolation with greedy weights

Mohammad Reza Khosravi[1,2] · Mehran Yazdi[3]

Received: 10 October 2017 / Accepted: 11 April 2018 / Published online: 23 April 2018

Abstract
In the digital world, watermarking technology is a solution for data hiding and completely essential for management and secure communications of digital data propagated over the internet-based platforms. Reversible watermarking is a quality-aware type of watermarking which has been applied in managing digital contents such as digital images, texts, audios and videos. Reversible watermarking is also known as lossless watermarking due to its preservation of all details of host and hidden data. One of the important uses of this kind of watermarking is to manage medical data regarding DICOM images. In the recent years, a new type of reversible watermarking technology entitled interpolation-based reversible watermarking has been introduced, and we are going to enhance it for DICOM images by using a hybrid approach based on computing error histogram and by applying an image interpolation with greedy weights (adaptive weighting). In practice, simulation results clearly show better performance of the proposed scheme compared to the previous techniques using interpolation-based reversible watermarking on different DICOM images.

Keywords Reversible watermarking · Digital Imaging and Communications in Medicine (DICOM) · Interpolation-Based Reversible Watermarking (IBRW) · Error histogram · Greedy Weights in Quartered Interpolation (GWQI) · Differential Expansion (DE)

1 Introduction

Nowadays, the most of Hospital Data Management Systems (HDMSs) and medical imaging systems are working on an internet-connected platform. Medical images such as CT, MRI, and PET are taken and stored digitally; in addition, these contents can be exchanged through a digital communication network. The images are very effective and important in the healthcare diagnostic processes because they have been used to show features of patients such as anatomical cross sections of internal organs and tissues; moreover, they are served by physicians to evaluate the patient's diagnosis and monitor the effects of the treatment [1]. So, protecting and managing medical images from a non-permissive usage are necessary and inevitable. Some impotent secure services require patient privacy and integrity of medical images which can intrinsically be provided using watermarking technologies. A watermark or hidden data are a part of information such as patient ID and the scrambled type of an image that can be hidden in the image without corrupting its specific details. The Digital Imaging and Communications in Medicine (DICOM) is a standard for storing, formatting and exchanging the medical images in medical hospitals and clinics; in addition, DICOM systems support the connectivity of printers networked to other digital devices via a local area network or internet, such as laser imagers. Digital images in medicine could be obtained from diagnostic modalities such as nuclear medicine, ultrasound,

✉ Mohammad Reza Khosravi
m.khosravi@sutech.ac.ir; m.r.khosravi.taut@gmail.com

Mehran Yazdi
yazdi@shirazu.ac.ir

[1] Department of Electrical and Electronic Engineering, Shiraz University of Technology, Shiraz, Iran

[2] Computer Engineering Department, Persian Gulf University, Bushehr, Iran

[3] Department of Communications and Electronic Engineering, Shiraz University, Shiraz, Iran

X-ray, CR, digital radiography and hospital information system [1]. The watermarking techniques can be used to create the image integrity and the private policy while preserving the diagnostic essential effects in the medical image [2]. Reversible watermarking embeds data within a medical image in the way that the original image can be completely restored; namely, this technology is a highly quality-aware way which protects the original quality of the host image as well as embedded data. Thus, many recent researches propose to use it for providing medical image integrity and patient privacy. In this paper, a secure approach with using a hybrid scheme based on error histogram and greedy weights image interpolation is proposed to support DICOM security. In practice, the simulation results clearly show better performance of the proposed method for different medical images than some previous interpolation-based reversible watermarking techniques. Our approach in this paper is to change the core interpolator of the method presented in [3]; however, we will keep the default interpolation template of the basic scheme (-known as quartered interpolation (QI)). In practice, the experimental results clearly show superior performance of the proposed method compared to the method proposed in [3] as well as recent interpolation-based reversible watermarking techniques. The rest of the paper is organized as follows. In second part, we review some approaches for computing error histogram under the histogram modification [2] and specifically DE-based reversible watermarking [4]. Section 3 represents details of interpolation-based reversible watermarking (IBRW). In Sect. 4, we introduce our proposed scheme. Section 5 of the article is allocated to performance evaluation of the proposed scheme for DICOM images and some benchmarks, and final section is conclusion and future developments.

2 Interpolation and differential expansion-based reversible watermarking

In 2010, Luo et al. [3] proposed a novel reversible algorithm named as interpolation-based reversible watermarking (IBRW) technique for digital watermarking based on computing histogram of interpolation error. This basic approach has been well cited, so we selected it as basic work. This algorithm is a reversible watermarking scheme which can hide and recover bits of watermark data. Luo et al.'s scheme is classified as a differential expansion-based (DE-based) watermarking technology [4] and can also be combined with other techniques like histogram shifting. In practice, this new approach could concurrently create both formal aims of hiding data and good quality of watermarked images. Lately, same methods such as algorithms in [5–7] worked on developing IBRW algorithm by modifying histograms of computed error images. For instance in [5], a new IBRW algorithm based on interpolation error histogram shifting has been proposed. In [6], the local prediction is used for DE-based reversible watermarking in the way that for each pixel, a least square predictor is computed based on a square block centered on a pixel and the corresponding prediction error is expanded. Also in [7], the authors have proposed an improved adaptive prediction method with using the auto-regression model and a general prediction error histogram modification framework for reversible data hiding. These recent schemes could improve some factors of watermarking performance; however, modifying, shifting and changing histogram are common solutions for the purpose and even can be used in other types of reversible watermarking. For example, methods in [8, 9] are the approaches in respect to histogram modification in both frequency and spatial domain, for more details refer to them. In fact, working on core interpolation of IBRW is the aim of our research which is completely new in its type (when method in [3] is used for hiding process). In the other words, we are going to change the core interpolator of the basic IBRW algorithm for enhancing watermarking performance because the basic theories of IBRW are independent from any interpolation algorithms [10–18], so in the following sections, firstly, we represent these foundations (Sect. 3) and then introduce our approach (Sect. 4).

In addition to the idea of IBRW, some other researchers have worked on interpolation-based reversible data hiding in different forms, such as methods in [19–21] which have different hiding processes. In [19], the authors have proposed an image interpolation-based reversible data hiding scheme using pixel value adjusting feature. Their method has two phases, image interpolation and data hiding, similar to IBRW algorithm and our scheme. In detail, it contains a new image interpolation method which is based on the existing Neighbor Mean Interpolation (NMI) and called Modified NMI (MNMI). The core interpolator in MNMI is based on classical methods such as simplified pixel averaging [19] with fixed weights. Thus, the method in [19] does not use an adaptive interpolator. In [20], another type of image interpolation-based reversible data hiding scheme has been proposed which uses Enhanced NMI (ENMI), and like [19], the interpolator is based on a simplified pixel averaging again. The authors in [21] have proposed a modified technique based on difference expansion, interpolation and histogram shifting where interpolation is a main part in it; however, a disadvantage of their technique is the use of a heuristic interpolator in spatial domain, which is not efficient in solving the interpolation problems generally and is only efficient in the specific watermarking problem investigated by the authors.

On the other hand, in the field of creating reversible watermarking and data hiding algorithm for medical images, there are some researches such as methods in [22–24]; however, their authors have not used interpolation in design of their approaches. Also, many other related works are available [25–32], for example, in [32], a novel technique for medical images has been proposed which focuses on histogram shifting, not a core interpolator. However, we consider an existing histogram processing block in our work in which it is not our novelty [5]. Therefore, as a novel approach, we wish to use the interpolation algorithms in the application of watermarking for medical images.

Clearly, our focus in this work is to propose a new interpolation method in the IBRW scheme to improve its performance in data hiding of medical images. Our contribution in this work is based on the fact that using an adaptive interpolator in IBRW can greatly improve the performance of watermarking algorithm, because the interpolator can be considered as a type of independent processing along with the data hiding process. The impact of the core interpolator will be discussed more in continuation, where we first introduce the original IBRW and then bring our new interpolator which can be integrated to IBRW.

3 Interpolation-based reversible watermarking (IBRW): backgrounds

IBRW algorithms like all watermarking algorithms have two steps: embedding process and extraction process. In continuation, both steps are reviewed.

3.1 Embedding process

Assume that we have an original host image x (matrix x). In addition, suppose x' is interpolated version of x created by using a predetermined interpolation algorithm. Thus, an error image (error matrix) is defined by differentiation of x and x' as follows [according to Eq. (1)].

$$e = x - x'. \tag{1}$$

When histogram of e is figured, four parameters are defined based on the figured histogram. We introduce these four parameters as follows. Figure 1 clearly shows the parameters LN, LM, RM and RN where LN (LN > 0) and RN are the lowest and the highest local minimum intensities, respectively, and LM and RM are first two local maximum intensities, according to the figure, it is observable that LN $<$ LM $<$ RM $<$ RN.

In Fig. 1, it is assumed that "Hist (LM)" is greater than "Hist (RM)," namely maximum value of "Hist (e)" is for a lower intensity (here, LM) but in practice LM $>$ RM is possible, so in these cases LM and RM values can be exchanged and it cannot affect the generality of our discussion. Based on these four parameters, there is a reversible function "Rev" that a specific error image e' by using this function can be computed (for more information about the "Rev" function refer to [3, 9]). Therefore, e' will be computed as Eq. (2).

$$e' = \mathrm{Rev}(e,\ b,\ \mathrm{LM}, \mathrm{LN}, \mathrm{RM}, \mathrm{RM}). \tag{2}$$

In the above equation, all values of e, b, LN, LM, RM and RN are previously known and computed based on the host image x, and b is a sample bit for hiding. Watermarked image is denoted by x'' and is calculated by Eq. (3), as below.

$$x'' = x' + e'. \tag{3}$$

In fact, x'' is output of the embedding process (hiding process) and contains hidden data. (Embedded data are a string of bits in IBRW algorithm.) IBRW algorithm is a bilateral algorithm; namely, at first, some of pixels have no changes and the rest of them will be candidate for hiding the data according to above explanations, and then in next step, these two groups of pixels are substituted with each other. (In [3], the authors have named two groups sample and non-sample pixels, see more information in the reference.) All processes of these two steps are repeated to complete hiding process in each hiding level (1-layer hiding).

In this scheme, hidden data are added to LM and RM pixels as the Least Significant Bit (LSB) of the pixels. As a matter of fact, pixels whose gray-level values are equal to LM or RM are detected for data hiding. It is performed in order to protect visual details of the watermarked image x'' for better perception and interpretation in Human Visual System (HVS). Due to the fact that some corresponding pixels in x and x' may be similar in gray-level value, error image for these pixels produces zero values. Thus, the mentioned pixels are not surely candidate for adding hidden bits because both LM and RM are bigger than LN under the constraint of LN > 0. The candidate pixels are the ones with similar gray-level values to LM and RM, so we can easily determine these candidates from x'' by knowing LM and RM and consequently generate x'. Therefore, there is no need to have original host image x which makes this scheme a blind watermarking method [33]. The impact of interpolator is significantly seen in selecting the more number of LSB pixels for hiding bits; namely, better selection of LM and RM completely depends on the core interpolator used. Of course that the location of LSB pixels is not previously defined and is according to the mentioned details in hiding process; however a good interpolator can effectively improve the IBRW performance.

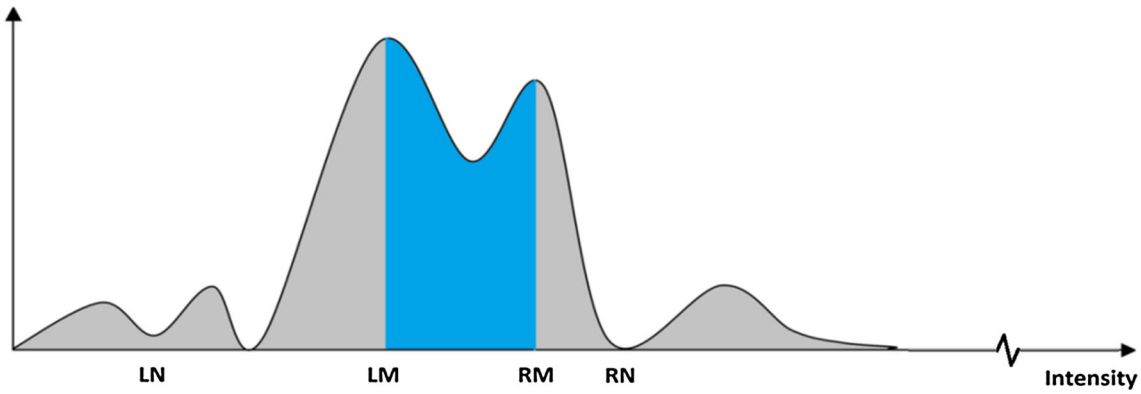

Fig. 1 A typical histogram for an error image (with hyperbole for better perception); in order to simplicity in showing the histogram and better perception, $e = |x - x'|$ is considered

3.2 Extraction process

At the receiver side, x'' is received. Also it is assumed that values of four parameters LN, LM, RM and RN as basic features of the host image x are existent from before. In addition to the mentioned parameters, the receiver has x'' which has been received from the sender and knows the "Rev" and interpolation algorithm details to extract the hidden data b. Thus, the receiver can extract b and x by using x'', LN, LM, RM, RN and reverse function of the "Rev." According to Eq. (4), b and e are directly obtained from the reverse function (see [3] for more details).

$$[e, b] = \text{Rev}^{-1}(x'', \text{LM}, \text{LN}, \text{RM}, \text{RM}). \tag{4}$$

In addition to the extraction formula of hidden data b (shown in Eq. (4)), we must restore x at the receiver side, and for availability of x' at receiver side, it is sufficient that we use Eq. (1) and rewrite it according to Eq. (5).

$$x = e + x'. \tag{5}$$

It is explicit that x is easily computable by Eq. (5), so both original host image x and hidden data b are 100% extractable; namely, IBRW algorithm is a success reversible watermarking algorithm based on computing histogram of interpolation error.

4 Proposed algorithm

In this section, we present the proposed scheme using Greedy Weights in Quartered Interpolation (GWQI) for computing error histogram in IBRW. As a matter of fact, IBRW is not depending on a specific interpolation technique [5], so we can easily integrate any interpolation technique in IBRW without changing other parts of its scheme. In [3, 5], the authors have used a quartered interpolation based on a famous interpolation technique entitled Linear Minimum Mean Square Error-estimation (LMMSE) [11, 12, 14]. In this way, x' will be reconstructed by using only 25% of the original pixels of x. In the case, interpolation can be known as an interpolation process with ratio 1:3 or a quartered interpolation where 75% of pixels in x' do not have originality. In the other words, they are reconstructed based on an interpolation algorithm. It is obvious that number of pixels which have originality in x' can be less or more than 25%. In this second case, interpolation algorithm is a non-quartered interpolation. Like the previous researches [3, 5], we use the quartered template in the current study; however, we change the weighting of LMMSE algorithm according to a new interpolation algorithm. Our new algorithm entitled Adaptive LMMSE (ALMMSE) has been successfully tested in different types of images; its details will be explained as follows. ALMMSE algorithm uses four free weights for each nonexisting pixel which are adaptively computed based on four near neighbors of the nonexisting pixel (sometimes, six neighbors are used in some cases, for more information see [17]), whereas the original algorithm (LMMSE) only computes two adaptive weights for each set of four pixels; namely, LMMSE mandatorily selects equal weights for some pixels and it is not clearly fair in comparison with ALMMSE.

First version of LMMSE interpolation algorithm [11] which was named Directional LMMSE (DLMMSE) by [13] was proposed by Zhang et al. in 2005 in order to apply in color demosaicking problems. After this, Zhang et al. have proposed a better version of DLMMSE in 2006 [12], and this version had been directly used in interpolation problems. This new version uses an approach based on directional filtering and data fusion to design the new LMMSE-based interpolator. In addition, a simplified version in terms of lower complexity and real-time application

was proposed in [12] (in [3, 16, 17], it has been named directional filtering and data fusion or DFDF interpolator too). LMMSE interpolator needs a pre-interpolator based on cubic convolution (CC) [10] or bilinear (BL) [10] when is used for a resizing problem because without the pre-interpolator, LMMSE is even worse than the CC interpolator, in this respect see [15]. Anyway, using LMMSE and also our ALMMSE as the core interpolator of IBRW does not need the mentioned pre-interpolators because there is no resizing problem and, moreover, LMMSE and ALMMSE are surely real-time processes. As follows, we discuss more about the quartered template and differences between LMMSE and ALMMSE. LMMSE idea is generally applicable for several processes in image processing such as demosaicking, resizing and noise removal which has been discussed in [14]. Figure 2a clearly shows the quartered template for the interpolation using the idea of LMMSE. In fact, LMMSE or any other interpolator in spatial domain determines details of selecting values of neighbors' weights, and it is an optimization problem. (For a frequency domain approach, see [31].) It was mentioned that LMMSE selects same values for some weights mandatorily. Assume that a, b, c and d are values of four near neighbors of a target/nonexisting pixel p (a pixel that needs reconstruction) where all of them have originality, in addition, positions of a, b, c, and d are according to Fig. 2b, c in which these parts show two general scenarios of pixel estimation (45°/135° and 0°/90°, respectively), see more details of them in our previous work toward image fusion based on LMMSE estimator [34]. LMMSE presents an optimization problem as Eq. (6).

$$\begin{aligned} & p' \overset{\text{LMMSE}}{=} w_1 \frac{a+c}{2} + w_2 \frac{b+d}{2} = \frac{w_1}{2}a + \frac{w_2}{2}b + \frac{w_1}{2}c + \frac{w_2}{2}d \\ & \{w_1, w_2\} = \underset{w_1+w_2=1}{\arg\min} \left[(p-p')^2\right] \\ & \underset{\text{for } i\neq j}{\overset{\text{Generally}}{w_i \neq w_j}} \end{aligned} \tag{6}$$

In above equation, p' is an estimation of the nonexisting value of p. It is observable that final weight of a is similar to c, and for b it is the same as that of d. The mentioned assumption is against greedy design of the interpolator because in practice for a real image, weights' values of two pixels corresponding a and c can be different. Thus, we propose using a full-adaptive structure for this optimization problem. Our suggestion is use of ALMMSE in the optimization problem of Eq. (7). In continuation of this section, we explain more details about selecting weights under ALMMSE.

$$\begin{aligned} & p' \overset{\text{ALMMSE}}{=} w_1 a + w_2 b + w_3 c + w_4 d \\ & \{w_1, w_2, w_3, w_4\} = \underset{w_1+w_2+w_3+w_4=1}{\arg\min} \left[(p-p')^2\right] \\ & \underset{\text{for } i\neq j}{\overset{\text{Generally}}{w_i \neq w_j}} \end{aligned} \tag{7}$$

A simple solution for selecting weights in the optimization problem is to select equal values for all weights (i.e., a quartered interpolation with fixed weights). It is explicit that this solution is completely far from the real response, but for accurate evaluation, we tested this solution too; however, its results were so weak which we will see in Sect. 5. For the mentioned scheme [Fixed Weights Quartered Interpolation (FWQI)], estimation of p is as

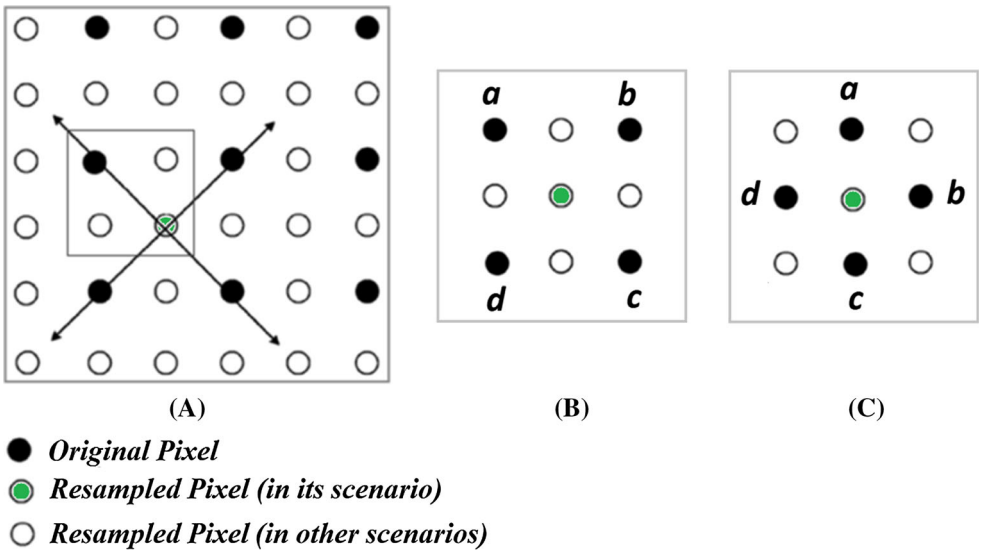

Fig. 2 **a** A representation for the quartered template used in LMMSE-based interpolators (original LMMSE and ALMMSE here), according to the figure, one-fourth of the pixels with black color are original, and the rest of them (three-fourths with color white) are reconstructed by four neighbors around each of them; **b**, **c** are general scenarios of estimation

Table 1 Qualitative comparison of some interpolation techniques discussed in this article in terms of different features, the table shows ALMMSE has the best features

	Quartered/ non-quartered	Greedy	Full adaptive	MRF-based	Real time	Complexity order	Qualitative performance
BL	Both	No	No	No	Yes (relatively)	Low	Low
CC	Both	No	No	No	No	High	High
FWQI	Quartered	Yes (relatively)	No	Yes (relatively)	Yes	Low	Very Low
LMMSE (DFDF)	Quartered	Yes	No	Yes (relatively)	Yes	Low	High
ALMMSE	Quartered	Yes	Yes	Yes	Yes	Low	High

Eq. (8). Table 1 shows a qualitative comparison among some mentioned interpolation techniques. In this table, a column is about to be "MRF-based." When an interpolator is MRF based, namely its estimation process considers that pixels in image have behaviors based on Markov random field (MRF), for more information about MRF-based interpolators, refer to [18].

$$\left.\begin{array}{r} w_1 = w_2 = w_3 = w_4 \\ w_1 + w_2 + w_3 + w_4 = 1 \end{array}\right\} \Rightarrow w_i \underset{i\in\{1,2,3,4\}}{\overset{\text{for}}{=}} 1/4 \Rightarrow p' \overset{\text{FWQI}}{=} 1/4(a+b+c+d) \tag{8}$$

Computing the coefficients w_1 to w_4 under ALMMSE is as Eq. (9). It is observable that a part in computation of the coefficients is to apply the output estimation in FWQI interpolator, i.e., p_{ave} which is the same of estimated p' by FWQI interpolator [Eq. (10)]. When using ALMMSE, there is possibility of selecting different values for all weights. For more discussions in this respect, refer to [17], however, there is all required information for complete implementation of ALMMSE in this paper.

$$\begin{aligned} w_1 &= \frac{(b-p_{\text{ave}})^2+(c-p_{\text{ave}})^2+(d-p_{\text{ave}})^2}{3\left[(a-p_{\text{ave}})^2+(b-p_{\text{ave}})^2+(c-p_{\text{ave}})^2+(d-p_{\text{ave}})^2\right]} \\ w_2 &= \frac{(a-p_{\text{ave}})^2+(c-p_{\text{ave}})^2+(d-p_{\text{ave}})^2}{3\left[(a-p_{\text{ave}})^2+(b-p_{\text{ave}})^2+(c-p_{\text{ave}})^2+(d-p_{\text{ave}})^2\right]} \\ w_3 &= \frac{(a-p_{\text{ave}})^2+(b-p_{\text{ave}})^2+(d-p_{\text{ave}})^2}{3\left[(a-p_{\text{ave}})^2+(b-p_{\text{ave}})^2+(c-p_{\text{ave}})^2+(d-p_{\text{ave}})^2\right]} \\ w_4 &= \frac{(a-p_{\text{ave}})^2+(b-p_{\text{ave}})^2+(c-p_{\text{ave}})^2}{3\left[(a-p_{\text{ave}})^2+(b-p_{\text{ave}})^2+(c-p_{\text{ave}})^2+(d-p_{\text{ave}})^2\right]} \end{aligned} \tag{9}$$

$$p_{\text{ave}} \overset{\text{Eq. (8)}}{=} \frac{1}{4}(a+b+c+d) \tag{10}$$

Now, we are going to combine IBRW algorithm with our ALMMSE and create a new IBRW algorithm. In the current study, we name the obtained approach IBRW-GW-QI, i.e., IBRW with Greedy Weights of Quartered Interpolation. Procedure of IBRW-GW-QI is according to Algorithm 1, as follows.

Algorithm 1. Steps in the proposed scheme, IBRW-GW-QI.

Sender side:

1) Get x (original host image).
2) Down-sample x.
3) Compute x′ by re-sampling x with using ALMMSE interpolator.
4) Compute e based on x and x′.
5) Compute RM, RN, LM, and LN based on Hist (e).
6) Embed b and compute x" according to Eq. (2) and Eq. (3).
7) Send x" (watermarked image) with RM, RN, LM, and LN to receiver.

Receiver side:

1) Get x", RM, RN, LM, and LN.
2) Down-sample x" based on a pattern similar to the sender.
3) Extract the factors b & e based on Eq. (4).
4) Re-sample x" by ALMMSE interpolator and generate x′.
5) Reconstruct x by x′ and e, according to Eq. (5).

In the next part, we will evaluate our proposed scheme in DICOM images [30] and some benchmarks. The methods evaluated in DICOM dataset in the current study are IBRW techniques with the quartered template but with different weighting, so we can name all of them IBRW-QI briefly. While using LMMSE (DFDF) interpolation [11, 12] (applied in the approach of Lou et al. in [3]), we name this scheme IBRW-DFDF.

5 Performance evaluation

For evaluation of the proposed method using MATLAB, in addition to DICOM images, two benchmarks, Lena and Baboon (Fig. 3), have been used. DICOM images are in both kinds of grayscale and color images and provided by [35–37]. First experiment investigates performance of the proposed IBRW-GW-QI algorithm in comparison with several significant algorithms based on the benchmarks in

(A) (B)

Fig. 3 Benchmarks for general evaluation of the proposed scheme in comparison with a wide range of recent watermarking techniques; results for part (**a**), Lena, are described in Table 2 and for part (**b**), Baboon, are in Table 3

Table 2 Results for Lena (for our algorithm, the results are an average of 10 tests; however, standard deviation of computed results is not considerable)

Schemes	Total Capacity (bit)	PSNR (dB)
Luo et al. [3] (IBRW-DFDF)	71,674	**48.82**
Zhang et al. [8]	**77,337**	35.21
Li et al. [46]	16,684	32.04
Lo et al. [47]	4025	33.36
Ou et al. [48]	68,000	48.90
Ni et al. [25]	5460	48.20
Hwang et al. [26]	5336	48.22
Hu et al. [27]	60,241	48.69
Proposed scheme (IBRW-GW-QI)	**72,196**	**48.78**

Bold values indicate relatively better results

Table 3 Results for Baboon (for our algorithm, the results are an average of 10 tests; however, standard deviation of computed results is not considerable)

Schemes	Total capacity (bit)	PSNR (dB)
Luo et al. [3] (IBRW-DFDF)	22,696	48.36
Zhang et al. [8]	44,204	28.38
Ou et al. [48]	22,000	**48.75**
Ni et al. [25]	5421	48.20
Hwang et al. [26]	5208	48.20
Hu et al. [27]	21,411	48.34
Proposed Scheme (IBRW-GW-QI)	**45,015**	**48.50**

Bold values indicate relatively better results

Fig. 3 and under the analysis using the approach discussed in [5].

The second experiment investigates performance of the proposed IBRW-GW-QI algorithm compared to IBRW-DFDF algorithm [3] by using 40 selected DICOM images. We remember the fact that both techniques are in type of IBRW techniques with the quartered template (IBRW-QI). Tables 2 and 3 show results of the first evaluations. These two tables clearly show that the proposed scheme outperforms other techniques in terms of simulation metrics. Metrics used for evaluation are peak signal-to-noise ratio (PSNR) in dB and capacity of hiding in different schemes in bit per pixel (bpp) unit. PSNR equation for two $N_1 \times N_2$ grayscale image f and f' with radiometric accuracy of d-pixel is as Eq. (11), and capacity of hiding is according to Eq. (12) generally. In all images, d is 8 (256 different gray levels).

$$\mathrm{PSNR} = 20\log\frac{2^d - 1}{\sqrt{\frac{1}{N_1 \times N_2}\sum_{i=1}^{N_1}\sum_{j=1}^{N_2}\left(f_{ij} - f'_{ij}\right)^2}} \tag{11}$$

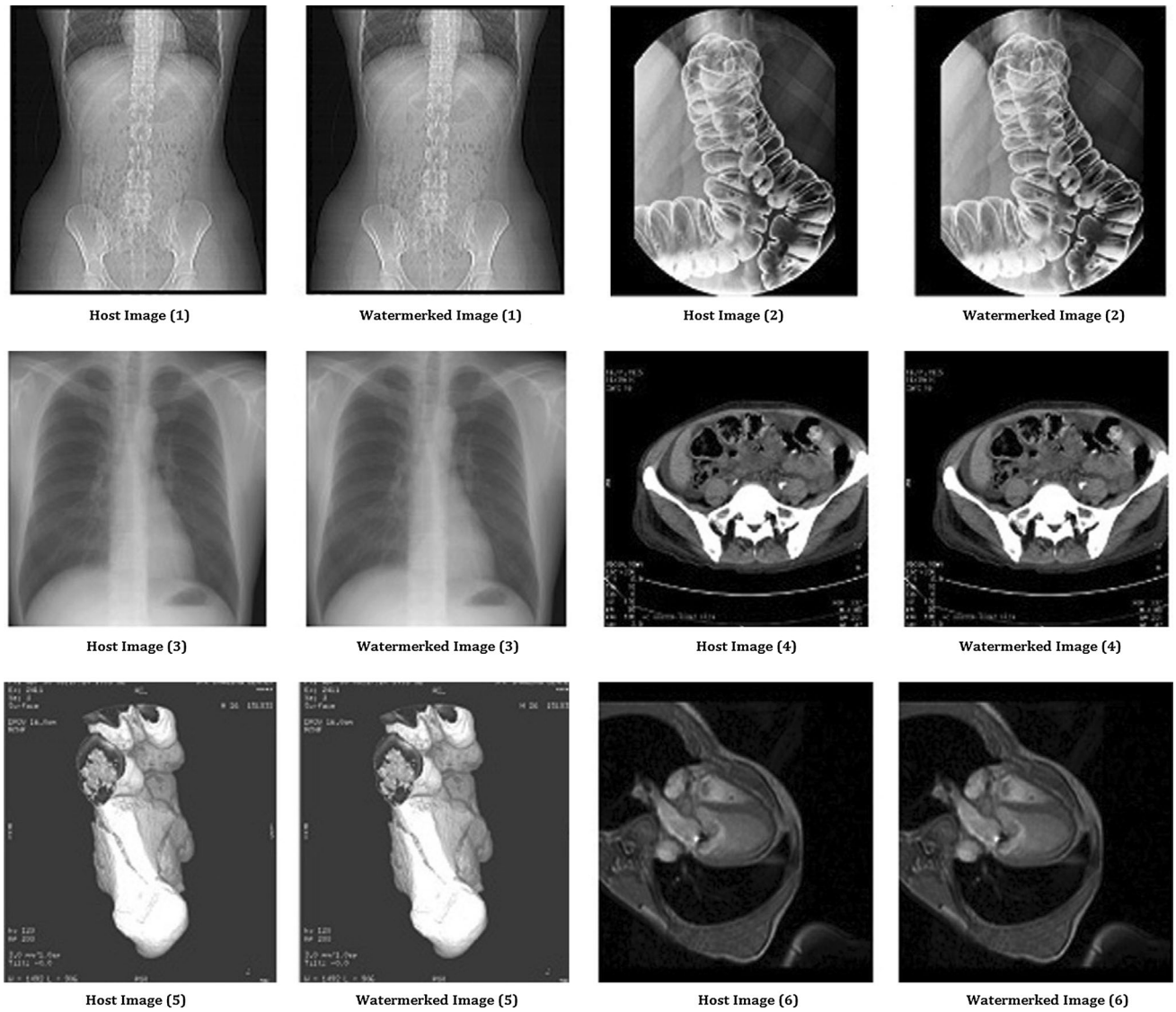

Fig. 4 Dataset for second evaluation contains 20 selected grayscale DICOM images from [35–37], six samples has been shown here

$$\text{Capacity (bpp)} = \begin{cases} \dfrac{\text{Number of embedded bits in the host}}{N_1 \times N_2} & \text{for a grayscale image} \\ & (a\ N_1 \times N_2 \text{ matrix}) \\ \dfrac{\text{Number of embedded bits in all layers of the host}}{N_1 \times N_2 \times M} & \text{for a color image with } M \text{ layers} \\ & (a\ N_1 \times N_2 \times M \text{ matrix}) \end{cases} \tag{12}$$

According to Table 3, the proposed algorithm absolutely outperforms other techniques; namely, better quality and higher capacity are simultaneously concluded while using the IBRW-GW-QI algorithm. In Figs. 4 and 5, some original host images from grayscale and color DICOM image dataset with processed images under the proposed watermarking algorithm are shown.

We do the second experiment similar to first one, but instead of the benchmarks, several DICOM images (20 grayscale and 20 color images from [35–37]) are used for the evaluation. At first, we observe the results of PSNR and capacity for three IBRW algorithms with different core interpolators (all are in type of QI) in Tables 4 and 5 (for grayscale and color images, respectively); these

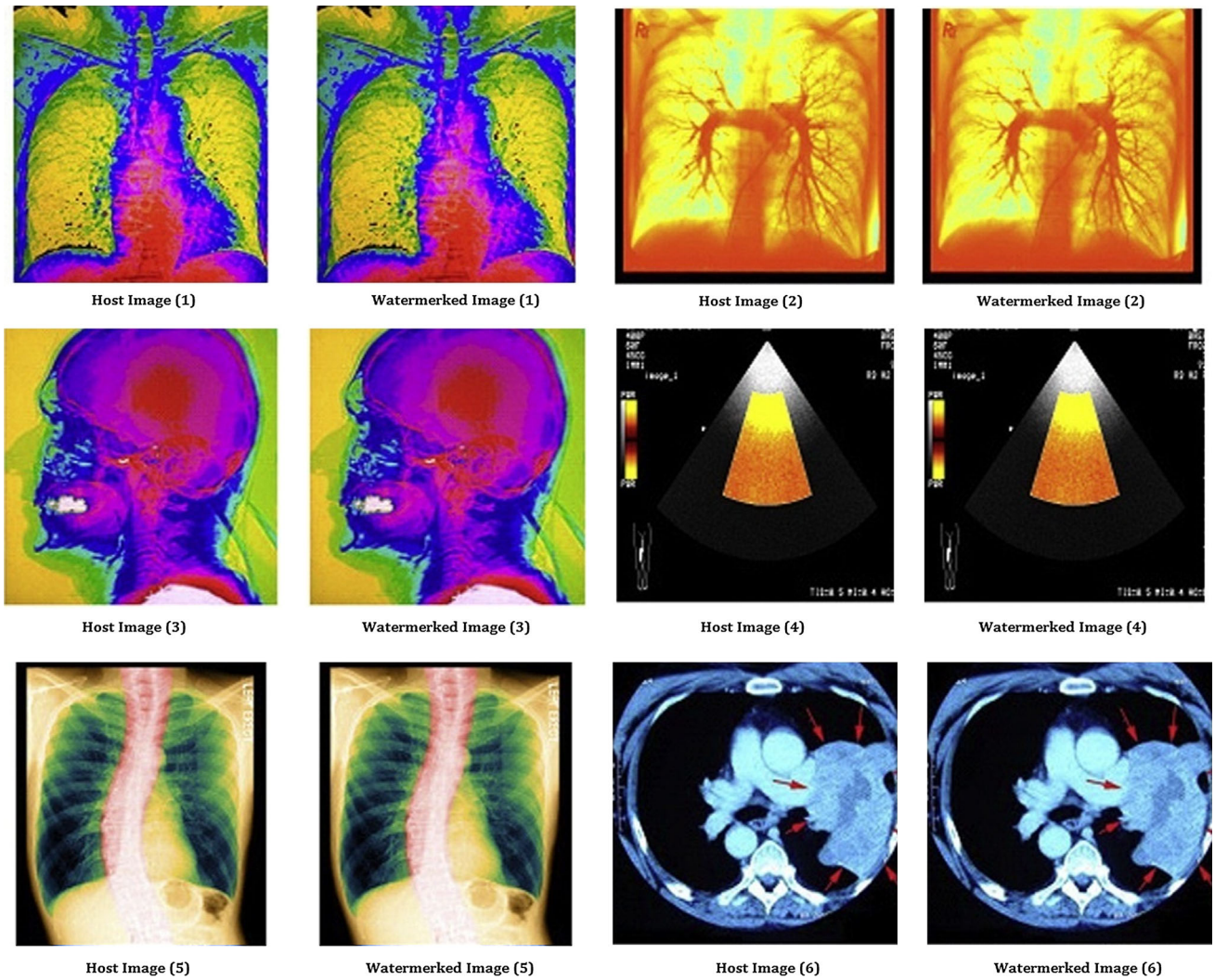

Fig. 5 Dataset for second evaluation also contains 20 selected color DICOM images from [35–37]

Table 4 Results for some grayscale samples versus three IBRW approaches with different quartered interpolators

The evaluated methods	Average capacity (bpp)	Average PSNR (dB)
IBRW-FW-QI (IBRW-QI with fixed weights interpolation)	0.64	28.2
IBRW-DFDF [3] (IBRW-QI with LMMSE (DFDF) interpolation)	0.75	31.8
Proposed scheme: IBRW-GW-QI (IBRW-QI with ALMMSE interpolation)	**0.78**	**31.9**

Bold values indicate relatively better results

Table 5 Results for some color samples versus IBRW approaches with different quartered interpolators

The evaluated methods	Average capacity (bpp)	Average MPSNR (dB)
IBRW-FW-QI (IBRW-QI with fixed weights interpolation)	0.63	28.1
IBRW-DFDF [3] (IBRW-QI with LMMSE (DFDF) interpolation)	0.75	31.7
Proposed scheme: IBRW-GW-QI (IBRW-QI with ALMMSE interpolation)	**0.78**	**31.8**

Bold values indicate relatively better results

tables show that the results of IBRW-QI with fixed weights interpolator (IBRW-FW-QI) are the weakest, so we ignore this approach in the next experiments. Figures 4 and 5 qualitatively show acceptable visual quality of the watermarked images under the proposed algorithm. Color images are in RGB color space and each channel of color is an

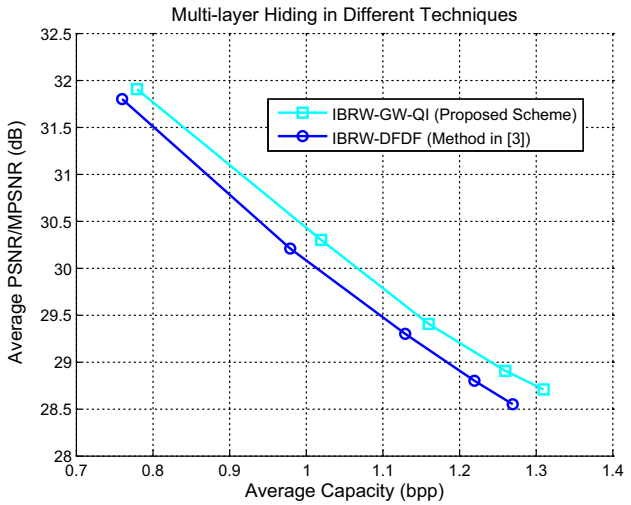

Fig. 6 Proposed algorithm (IBRW-GW-QI) is clearly better than IBRW-DFDF in terms of PSNR/MPSNR index for both types of grayscale and color images in different times of running the embedding process

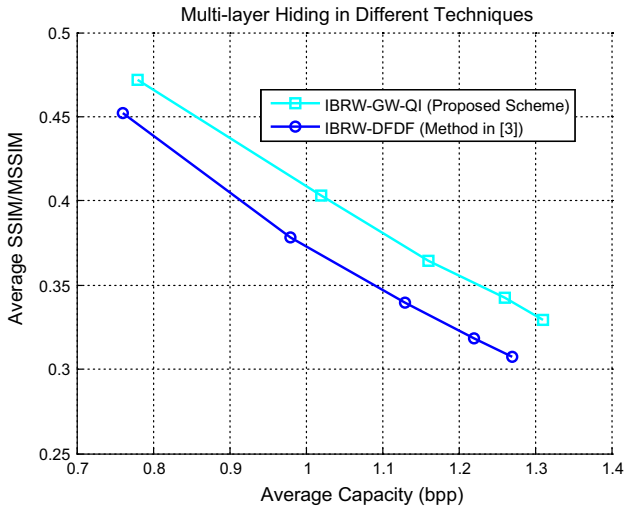

Fig. 7 Proposed algorithm (IBRW-GW-QI) is clearly better than IBRW-DFDF in terms of SSIM/MSSIM index for both types of grayscale and color images in different times of running the embedding process

8-bit image ($d = 8$). In the color images, PSNR is converted to a general form which considers all color channels; this form is known as MPSNR (M-layer PSNR). MPSNR has been shown in Eq. (13); it is noticeable that M for a RGB image is 3. In these new evaluations related to second experiment, the proposed algorithm outperforms IBRW-DFDF again.

$$\mathrm{MPSNR} = 20 \log \frac{2^d - 1}{\sqrt{\frac{1}{N_1 \times N_2 \times M} \sum_{i=1}^{N_1} \sum_{j=1}^{N_2} \sum_{k=1}^{M} \left(f_{ijk} - f'_{ijk}\right)^2}} \tag{13}$$

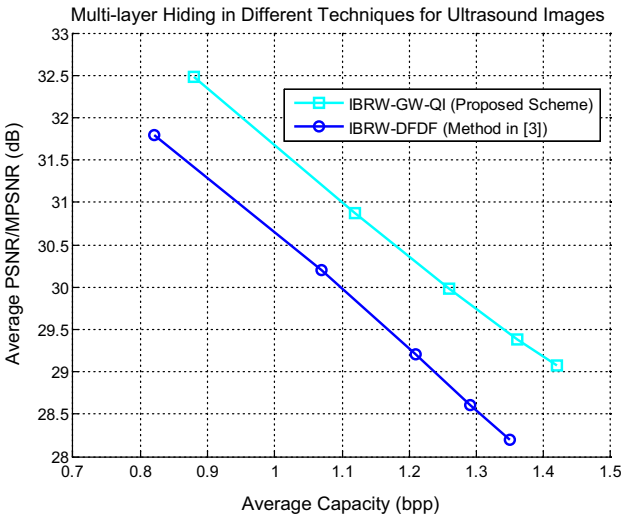

Fig. 8 Evaluation of the mentioned schemes in ultrasound images, the proposed scheme is strongly better than IBRW-DFDF

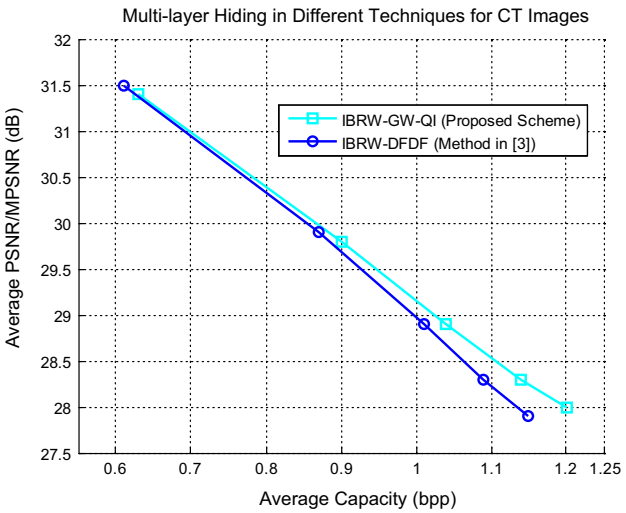

Fig. 9 Evaluation of the mentioned schemes in CT images, the proposed scheme is relatively better than IBRW-DFDF, specifically in higher iterations of multilayer hiding

All results in Figs. 4 and 5 were obtained after only one-time running the embedding process in both watermarking algorithms. Now, we are going to continue times of running the embedding process for both schemes. In this case, results create 2-D curves which are shown in Fig. 6 for the mentioned schemes and for all grayscale and color DICOM images in terms of PSNR/MPSNR. Similarly, Fig. 7 represents an evaluation like Fig. 6 in which it uses Structural Similarity (SSIM) or M-layer SSIM (MSSIM) instead of PSNR/MPSNR. It is notable that SSIM is a newer image quality assessment index and can cover and solve some weaknesses of PSNR; in order to read more things about it and its superiority than PSNR, refer to [34]. When we have

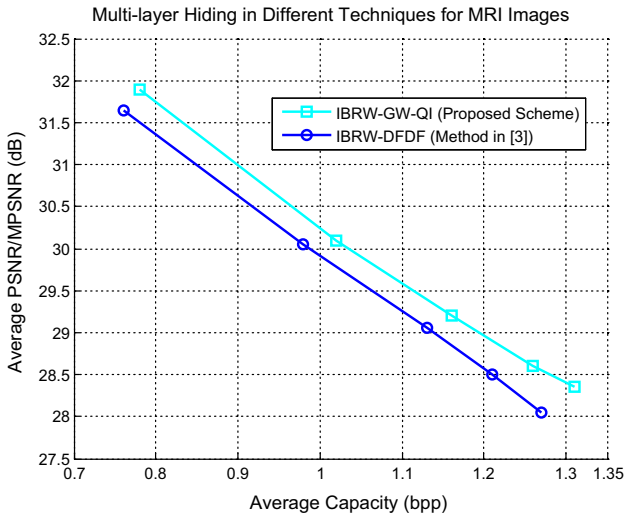

Fig. 10 Evaluation of the mentioned schemes in MRI images, the proposed scheme is strongly better than IBRW-DFDF

RGB image, MSSIM $= (\sum_{1:3} \text{SSIM})/3$.For generality, PSNR and MPSNR are combined together, and an average of both is used in the figure. Besides, Figs. 8, 9 and 10 show detailed results for different types of grayscale/color DICOM images (ultrasound, CT, and MRI, respectively). These figures show relatively better performance of the proposed scheme in comparison with IBRW-DFDF and for different types of medical images.

6 Conclusion and future developments

One of the important uses of this kind of reversible watermarking is managing DICOM images. In this paper, we firstly reviewed details of a new strategy in watermarking entitled IBRW which uses interpolation process in itself, and then we discussed about the quartered interpolators. Finally, we introduced a new watermarking algorithm which uses IBRW strategy with ALMMSE interpolator and named our scheme IBRW-GW-QI. The proposed scheme could prove the use of a better interpolator in the structure of IBRW creates better performance in terms of PSNR results and hiding capacities. For future work, researchers can investigate about using a bilateral non-quartered interpolator as core interpolator of IBRW. Besides, applying IBRW with a better interpolator and histogram modifiers like [28, 29] for achieving improved results is another idea for future studies. Creating an applied version for multimedia and real-time wireless sensor networks [38, 39] is also another selection. Combining the approach with new image encryption techniques, such as [40–42], toward joint encryption/watermarking can be a good idea. Developing IBRW approach toward other applications such as multi-band remote sensing images is also a novel idea for next researches. Joint medical image reconstruction/restoration/watermarking might also be considered with using novel approaches such as [43]. As a final proposition, we can do interpolation in the frequency domain [44] or combine the proposed approach with an existing watermarking technique which works in the frequency domain [45].

Acknowledgements The authors warmly thank Mohammad Arabzadeh for his support. In addition, we would like to thank all reviewers and editors for their helpful comments and efforts.

Compliance with ethical standards

Conflict of interest The authors declare that they have no conflicts of interest.

References

1. Abd-Eldayem M (2013) A proposed security technique based on watermarking and encryption for Digital Imaging and Communications in Medicine. Egypt Inform J 14:1–13
2. Lin C-C, Tai W-L, Chang C-C (2008) Multilevel reversible data hiding based on histogram modification of difference images. Pattern Recogn 41:3582–3591
3. Luo L, Chen Z, Chen M, Zeng X, Xiong Z (2010) Reversible image watermarking using interpolation technique. IEEE Trans Inf Forensics Secur 5(1):187–193
4. Arabzadeh M, Helfroush MS, Danyali H, Rahimi MR (2011) DE-based reversible medical image authentication using hamming code. In: International e-conference on computer and knowledge engineering (ICCKE), pp 183–188
5. Arabzadeh M, Danyali H, Helfroush MS (2010) Reversible watermarking based on interpolation error histogram shifting. In: International symposium on telecommunications (IST'2010), pp 840–845
6. Dragoi I, Coltuc D (2014) Local-prediction-based difference expansion reversible watermarking. IEEE Trans Image Process 23(4):1779–1790
7. Wen J, Lei J, Wan Y (2012) Reversible data hiding through adaptive prediction and prediction error histogram modification. Int J Fuzzy Syst 14(2):244–256
8. Zhang S, Gao T, Yang L (2016) A reversible data hiding scheme based on histogram modification in integer DWT domain for BTC compressed images. Int J Netw Secur 18(4):718–727
9. Tian J (2003) Reversible data embedding using a difference expansion. IEEE Trans Circuits Syst Video Technol 13(8):890–896
10. Gonzalez RC, Woods RE (2008) Digital image processing, 3rd edn. Prentice Hall, NJ
11. Zhang L, Wu X (2005) Color demosaicking via directional linear minimum mean square-error estimation. IEEE Trans Image Process 14(12):2167–2178
12. Zhang L, Wu X (2006) An edge-guided image interpolation algorithm via directional filtering and data fusion. IEEE Trans Image Process 15(8):2226–2238
13. Zhang L, Wu X, Buades A, Li X (2011) Color demosaicking by local directional interpolation and nonlocal adaptive thresholding. J Electron Imaging 20(2):023016
14. Getreuer P (2011) Zhang-Wu directional LMMSE image demosaicking. Image Process Line (IPOL) 1:117–126

15. Lee S, Kang M, Uhm K, Ko S (2016) An edge-guided image interpolation method using taylor series approximation. IEEE Trans Consum Electron 62(2):159–165
16. Baghaie A, Yu Z (2015) Structure tensor based image interpolation method. Int J Electron Commun (AEÜ) 69:515–522
17. Khosravi MR, Rostami H (2016) A new statistical technique for interpolation of landsat images. In: ICAUCAE 2016, SID Conference Publications, Tehran, Iran
18. Colonnese S, Rinauro S, Scarano G (2013) Bayesian image interpolation using Markov random fields driven by visually relevant image features. Sig Process Image Commun 28:967–983
19. Malik A, Sikka G, Verma H (2016) An image interpolation based reversible data hiding scheme using pixel value adjusting feature. Multimedia Tools Appl 76:13025–13046
20. Chang Y-T, Huang C-T, Lee C-F, Wang S-J (2013) Image interpolating based data hiding in conjunction with pixel-shifting of histogram. J Supercomput 66:1093–1110
21. Lu T-C, Chang C-C, Huang Y-H (2014) High capacity reversible hiding scheme based on interpolation, difference expansion, and histogram shifting. Multimedia Tools Appl 72:417–435
22. Golpira H, Danyali H (2011) Reversible medical image watermarking based on wavelet histogram shifting. Imaging Sci J 59:49–59
23. Lei B, Tan E, Chen S, Ni D, Wang T, Lei H (2014) Reversible watermarking scheme for medical image based on differential evolution. Expert Syst Appl 41:3178–3188
24. Rocek A (2016) A new approach to fully-reversible watermarking in medical imaging with breakthrough visibility parameters. Biomed Signal Process Control 29:44–52
25. Ni Z, Shi Y, Ansari N, Su W (2006) Reversible data hiding. IEEE Trans Circuits Syst Video Technol 16(3):354–362
26. Hwang J, Kim JW, Choi JU (2006) A reversible watermarking based on histogram shifting. Lecture notes in computer science. Springer, Berlin
27. Hu Y, Lee H, Li J (2009) DE-based reversible data hiding with improved overflow location map. IEEE Trans Circuits Syst Video Technol 19(2):250–260
28. Arabzadeh M, Rahimi MR (2012) Reversible data hiding scheme based on maximum histogram gap of image blocks. KSII Trans Internet Inf Syst 6(8):1964–1981
29. Arabzadeh M, Helfroush MS, Danyali H, Kasiri K (2011) Reversible watermarking based on generalized histogram shifting. In: 18th IEEE international conference on image processing (ICIP), pp 2741–2744
30. Tan CK, Ng JC, Xu X, Poh CL, Guan YL, Sheah K (2011) Security protection of DICOM medical images using dual-layer reversible watermarking with tamper detection capability. J Digit Imaging 24(3):528–540
31. Khalil MI (2017) Medical image steganography: study of medical image quality degradation when embedding data in the frequency domain. Int J Comput Netw Inf Secur 9:22
32. Kelkar V, Tuckley K, Nemade H (2017) Novel variants of a histogram shift-based reversible watermarking technique for medical images to improve hiding capacity. J Healthcare Eng. https://doi.org/10.1155/2017/3538979
33. Manimehalai P, Rani PAJ (2016) A new robust reversible blind watermarking in wavelet-domain for color images. Int J Image Graph 16(2):1650006
34. Khosravi MR, Sharif-Yazd M, Moghimi MK, Keshavarz A, Rostami H, Mansouri S (2017) MRF-based multispectral image fusion using an adaptive approach based on edge-guided interpolation. J Geogr Inf Syst 9(2):114–125
35. http://www.dicomlibrary.com
36. http://www.aycan.de/sample-dicom-images.html
37. http://dicom.nema.org
38. Alhihi M (2017) Determining the optimum number of paths for realization of multi-path routing in MPLS-TE networks. TELKOMNIKA 15(4):1701–1709
39. Khosravi MR, Basri H, Rostami H (2018) Efficient routing for dense UWSNs with high-speed mobile nodes using spherical divisions. J Supercomput 74(2):696–716
40. Wen W, Zhang Y, Fang Y, Fang Z (2018) Image salient regions encryption for generating visually meaningful ciphertext image. Neural Comput Appl 29(3):653–663
41. Khan M, Asghar Z (2018) A novel construction of substitution box for image encryption applications with Gingerbreadman chaotic map and S8 permutation. Neural Comput Appl 29(4):993–999
42. Khosravi MR, Rostami H, Samadi S (2018) Enhancing the binary watermark-based data hiding scheme using an interpolation-based approach for optical remote sensing images. Int J Agric Environ Inf Syst 9(2):53–71
43. Kala R, Deepa P (2017) Adaptive hexagonal fuzzy hybrid filter for Rician noise removal in MRI images. Neural Comput Appl. https://doi.org/10.1007/s00521-017-2953-4
44. Dianat R, Ghanbari M (2015) Comparison between various standard definition to high definition image conversion methods. Recent Adv Commun Netw Technol 4:6–15
45. Bazargani M, Ebrahimi H, Dianat R (2012) Digital image watermarking in wavelet, contourlet and curvelet domains. J Basic Appl Sci Res 11(2):11296–11308
46. Li CH, Lu ZM, Su YX (2011) Reversible data hiding for BTC-compressed images based on bit-plane flipping and histogram shifting of mean tables. Inf Technol J 10(7):1421–1426
47. Lo CC, Hu YC, Chen WL, Wu CM (2014) Reversible data hiding scheme for BTC-compressed images based on histogram shifting. Int J Secur Appl 8(2):301–314
48. Ou B, Li X, Zhao Y, Ni R, Shi YQ (2013) Pairwise prediction-error expansion for efficient reversible data hiding. IEEE Trans Image Process 22(12):5010–5021